

See discussions, stats, and author profiles for this publication at: <https://www.researchgate.net/publication/285696289>


# Iberomesornis romerali (Aves, Ornithothoraces) reevaluated as an Early Cretaceous enantiornithine

**Article** *in* Neues Jahrbuch für Geologie und Paläontologie - Abhandlungen · March 2000  
DOI: 10.1127/njgpa/215/2000/365

CITATIONS  
34

READS  
329

1 author:




**Paul C. Sereno**  
University of Chicago

132 PUBLICATIONS 10,694 CITATIONS

SEE PROFILE

Some of the authors of this publication are also working on these related projects:



Early dinosaurs from the Carnian-Norian Ischigualasto Formation, Northwestern Argentina [View project](#)

## ***Iberomesornis romerali* (Aves, Ornithothoraces) reevaluated as an Early Cretaceous enantiornithine**

**Paul C. Sereno**, Chicago

With 9 figures and 4 tables

---

SERENO, P. C. (2000): *Iberomesornis romerali* (Aves, Ornithothoraces) reevaluated as an Early Cretaceous enantiornithine. – N. Jb. Geol. Paläont. Abh., **215**: 365–395; Stuttgart.

**Abstract:** Recent cladistic analyses have placed the Early Cretaceous avian, *Iberomesornis romerali*, outside the enantiornithine radiation at the base of Ornithothoraces. This conclusion is based on erroneous interpretations of the holotypic skeleton, which is shown here to exhibit ten enantiornithine synapomorphies. Revised diagnoses are presented for Enantiornithes and *Iberomesornis romerali*, which is very close in skeletal form to the Spanish and Chinese enantiornithines *Concornis lacustris* and *Sinornis santensis*, respectively.

**Zusammenfassung:** Neuere cladistische Analysen anderer Autoren haben den Unterkreide-Vogel *Iberomesornis romerali* irrtümlich aus der Enantiornithinen-Radiation an der Basis der Ornithothoraces ausgeschlossen. Neue Untersuchungen zeigen aber, daß *I. romerali* in seinem Skelettbau den spanischen und chinesischen Enantiornithinen *Concornis lacustris* und *Sinornis santensis* sehr nahesteht.

---

### **Introduction**

The discovery of *Iberomesornis romerali* (SANZ et al. 1988) heralded a new era in avian paleontology during which skeletal remains from inland lacustrine mudstones, rather than marginal marine limestones, would come to dominate the early fossil record of birds. Soon after its discovery, *Ibero-*

*mesornis* was accorded an intermediate position in avian phylogeny (SANZ & BUSCALIONI 1992, CHIAPPE 1991 1995a, b, 1996a, b, SANZ et al. 1995, PADIAN & CHIAPPE 1998) - a position more advanced than *Archaeopteryx* but less advanced than Enantiornithes or more derived birds, here termed Euornithes (Figs. 1, 2).

In this paper, previous interpretations of the phylogenetic position of *Iberomesornis* are briefly reviewed (Fig. 1). Then the taxonomy and skeletal anatomy of the holotype are reviewed, and its phylogenetic position is reevaluated in light of the new descriptive evidence. Throughout this paper, the terms “Aves,” “Ornithurae,” “Enantiornithes,” and “Euornithes” are used in accordance with taxonomic definitions set forth in SERENO (1998) (Fig. 2).

**Previous interpretations**

**SANZ & BONAPARTE 1992**

The cladistic analysis presented by SANZ & BONAPARTE (1992) did not consider Enantiornithes, because of the fragmentary nature of the material pertaining to that group at that time (WALKER 1981). SANZ & BONAPARTE placed *Iberomesornis* among basal avians in a position more advanced than *Archaeopteryx* but less advanced than other well known Mesozoic avians (Fig. 1A). Although some of the evidence they used to place *Iberomesornis* in this basal position (e. g., only five sacrals, separate proximal and distal tarsals) is discussed and rejected below, their phylogenetic assessment of *Iberomesornis* and the taxa they considered would still be accepted today.

**SANZ & BUSCALIONI 1992**

SANZ & BUSCALIONI (1992) presented a cladistic analysis of basal avians to determine the relationships of *Iberomesornis*. They considered 14 characters and 5 ingroup taxa in their most basic analysis (Fig. 1B). The data matrix does yield their tree as the single most parsimonious solution, although one of their characters (character 9) is uninformative.

**Fig. 1.** Previous phylogenetic placement of *Iberomesornis romerali*. **A:** SANZ & BONAPARTE 1992; **B:** SANZ & BUSCALIONI 1992; **C:** SERENO & RAO 1992; **D:** KUROCHKIN 1996; **E:** CHIAPPE 1995 a, b, 1996 a, b.

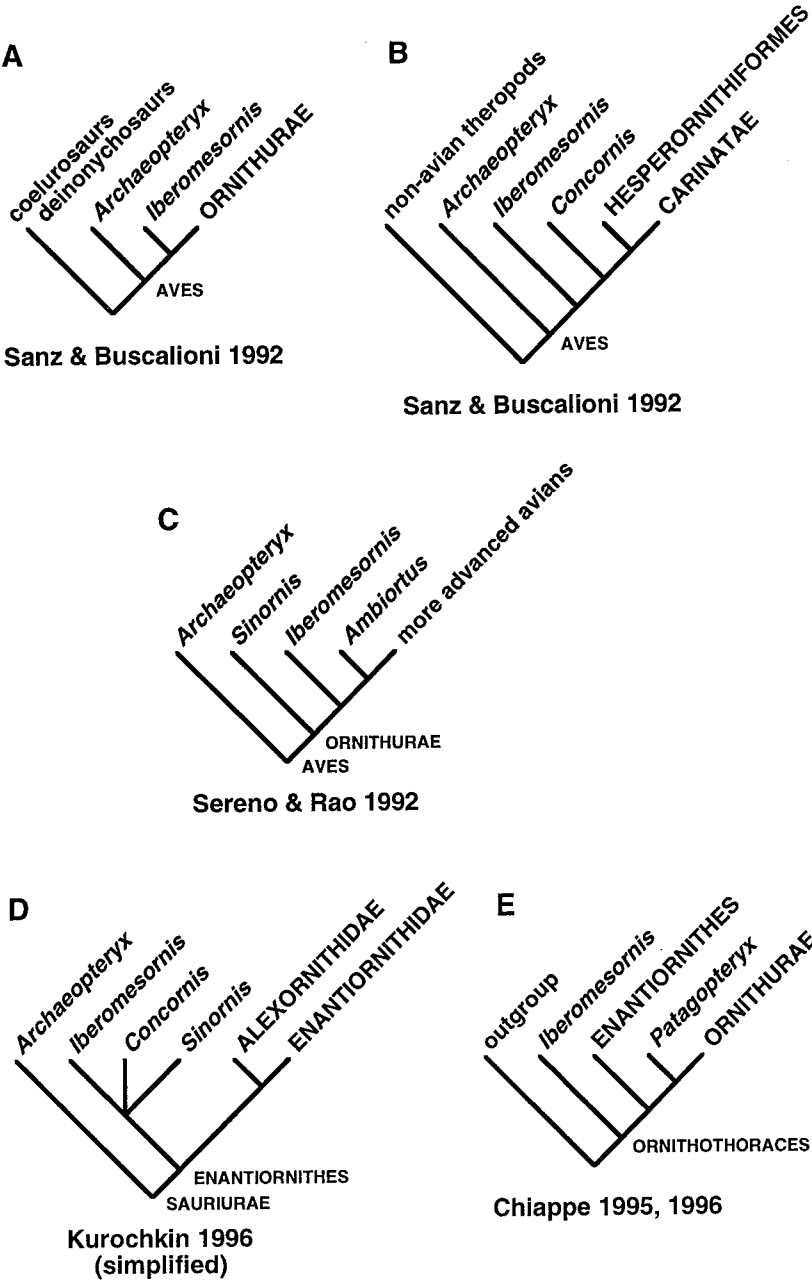


**Fig. 1** (Legend see p. 366)

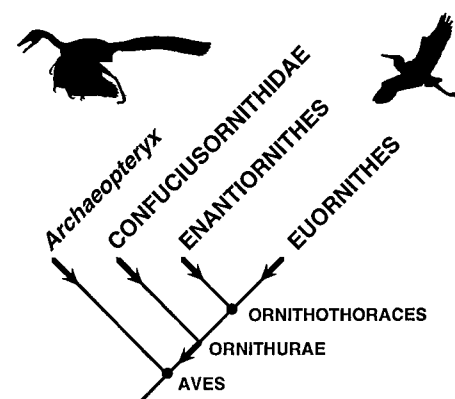


**Fig. 2.** Higher-level avian phylogeny and taxonomy used in this paper. Arrows and dots indicate node-based and stem-based taxa, respectively (after SERENO 1998). Confuciusornithidae is defined here as a stem-based taxon: All avians closer to *Confuciusornis sanctus* than Neornithes.

The synapomorphies of interest in this connection are those that unite the enantiornithine *Concornis* with more advanced avians to the exclusion of *Iberomesornis*. There are two unambiguous synapomorphies in their analysis at this node (characters 6 and 7). The first is the fusion of the tibia and proximal tarsals as a tarsometatarsus. The supposed absence of a coossified tarsometatarsus in *Iberomesornis* was also used by SANZ & BONAPARTE (1992) and later authors to position *Iberomesornis* below other ornithothoracines. The second character, the presence of a “fan-like” expansion of the distal condyles of the metatarsus with “trochlear structure” (SANZ & BUSCALIONI 1992:839), is poorly defined and has not been used by subsequent authors. The principal evidence, therefore, to support the basal position of *Iberomesornis* relative to *Concornis* resides with the absence of a tarsometatarsus in *Iberomesornis*. SANZ & BUSCALIONI (1992) included Enantiornithes in a subsequent analysis, but the high level of missing data for this taxon in their analysis yielded inconclusive results.

## SERENO & RAO 1992

SERENO & RAO presented an analysis of basal avians that compared *Iberomesornis* and *Sinornis*. They did not include Enantiornithes in the analysis or make any statements regarding the relationship of that group to *Iberomesornis* and *Sinornis*, contrary to remarks by CHINSAMY et al. (1995: fig. 3), CHIAPPE (1995a:352), and PADIAN & CHIAPPE 1998:29). Enantiornithes at that time, were known from disarticulated bones belonging to several taxa that remain poorly known (WALKER 1981).

SERENO & RAO (1992: fig. 5) placed *Iberomesornis* at a more advanced position among basal avians than *Sinornis* (Fig. 1C) on the basis of two derived characters, the absence of gastralria and the rod-shaped form of the proximal coracoid. It is now clear, however, that *Sinornis* also shares both of these features. The structures that appeared to represent gastralria (SERENO & RAO 1992: fig. 4) are the distal ends of slender posterior dorsal ribs that pass into, and out of, the plane of the acid-prepared half of the holotypic skeleton (SERENO et al. in press). Thus there is no evidence for gastralria in *Sinornis*, and this reinterpretation is confirmed by the absence of gastralria in additional specimens (= *Cathayornis*; ZHOU 1995). The original interpretation of the coracoid was based on the proximal end of the left humerus, as seen in cross-section on the original part slab (SERENO & RAO 1992: fig. 1). The acid-prepared cast suggests that the coracoid in *Sinornis* is also rod-shaped proximally, as confirmed in additional specimens (= *Cathayornis*; IVPP V9769). In summary, two synapomorphies that placed *Iberomesornis* in a more advanced position relative to *Sinornis* (SERENO & RAO 1992) are regarded here as errors of interpretation of the holotypic skeleton of *Sinornis*.

## KUROCHKIN 1995, 1996

Although KUROCHKIN (1995:51) listed several features to justify his conclusion that *Iberomesornis* is an enantiornithine (Fig. 1D), the only one that is regarded here as an enantiornithine synapomorphy is the canted angle of the distal humeral condyles (“transversely placed external condyle of the humerus more proximal than the pronounced internal condyle”). With the possible exception of lateral fossae on the dorsal centra, the other features KUROCHKIN listed are either plesiomorphic or amount to erroneous interpretations of the holotypic skeleton of *Iberomesornis*. The presence of an “enlarged pygostyle” is plesiomorphic, as shown in the many specimens of the more basal avian *Confuciusornis*. An intrafurcular angle of less than 70° (“sharp-angled furcula”) is also common within Euornithes, the sister taxon to Enantiornithes (Fig. 2). “Rapprochement of the proximal ends of the

metatarsals", if meant as a reference to their coossification, is not unique to Enantiornithes but rather characterizes all ornithurines. The absence of a tibiotarsus and distal tarsal "cap" on the metatarsals, on the other hand, are regarded here as observational errors, because a tibiotarsus and tarsometatarsus are present in *Iberomesornis*. Even if the tarsals were not fused in *Iberomesornis*, the absence of coossification cannot be used as evidence of enantiornithine affinity.

In a subsequent cladistic analysis, KUROCHKIN (1996) placed *Iberomesornis* within Enantiornithes. Many of his supporting synapomorphies, however, are ill defined and cannot function as derived characters in support of his cladogram. "Metatarsals II-IV elongate and gracile" and "coracoidal shaft elongate and gracile", for example, are too vague to be meaningful and could not support Enantiornithes as synapomorphies even if they were better defined. In summary, although KUROCHKIN (1995, 1996) placed *Iberomesornis* within Enantiornithes, he did not discuss the evidence originally proposed for its exclusion from Enantiornithes and did not present convincing character evidence for its inclusion.

#### MARTIN 1995

MARTIN (1995:27) classified *Iberomesornis* within Enantiornithes but did not discuss in detail his evidence for this assignment. The features he mentioned to support this assignment included a "broad flat furcula with a large hypocleideum" and a "hypertrophied" ungual on pedal digit I.

#### CHIAPPE 1991, 1995 a, b, 1996 a, b, 1997

CHIAPPE (1991, 1995 a, b, 1996 a, b, 1997) has provided the principal support for the basal position of *Iberomesornis* among ornithothoracines (Fig. 1 E), a phylogenetic arrangement followed by CHIAPPE et al. (1996), SANZ et al. (1995, 1996), and FORSTER et al. (1998). Nine unambiguous synapomorphies have been used in several of these analyses to unite ornithothoracines to the exclusion of *Iberomesornis*: (1) eight sacral vertebrae, (2) heterocephalous cervical vertebrae, (3) prominent ventral processes on cervicodorsal vertebrae, (4) scapulocoracoid articulation well below the shoulder end of the coracoid, (5) humeral transverse ligamental groove well developed, (6) humeral distal condyles mainly on cranial aspect, (7) pelvic girdle coossified, (8) coossification of the tibiotarsus, and (9) coossification of the tarsometatarsus. This evidence is discussed below in the light of new descriptive information from the holotypic skeleton.

#### Systematic paleontology

Aves LINNE 1758

Ornithurae HAECKEL 1866

Ornithothoraces CHIAPPE & CALVO 1994

Enantiornithes WALKER 1981

Definition: All ornithothoracines closer to *Sinornis* than Neornithes (SERENO 1998).

Revised diagnosis: Enantiornithes, as currently known, are characterized by the following 27 postcranial autapomorphies: **1**, parapophyses of the anterior dorsals centrally positioned on centrum (lateral view); **2**, sternal slot for hypocleideum; **3**, furcular dorsolateral rami L- or V-shaped in cross-section; **4**, hypocleideum length 40 % or more dorsolateral ramus of furcula; **5**, scapular acromial process quadrangular; **6**, scapular acromial process deflected medially 45° from the long axis of the scapula; **7**, scapulocoracoid articulation with scapular pit and coracoid tuber; **8**, coracoid ventral ramus with convex lateral margin; **9**, coracoid ventral ramus transversely arching; **10**, humeral head saddle-shaped; **11**, humeral internal tuberosity with pneumatic opening on posterior aspect; **12**, humeral internal tuberosity with circular fossa on medial extremity; **13**, humeral anterior trochanter; **14**, humeral posterior trochanter formed as a pendant process with a subtriangular cross-section and terminal fossa; **15**, humeral anterior fossa just distal to proximal articular end; **16**, humeral ulnar condyle (anterior view) flat, subrectangular; **17**, humeral distal condyles with transverse axis angled ventromedially at approximately 25° from the perpendicular to the shaft axis; **18**, humeral distal end with maximum width across the epicondyles three times maximum anteroposterior depth; **19**, manual II-1 with pneumatic foramen; **20**, iliac postacetabular process with maximum depth one-third the maximum depth of the preacetabular process; **21**, tibial cnemial crest anteromedially positioned; **22**, metatarsal I distal condyles reflected posteriorly (1); **23**, metatarsal I distal condyles joined along dorsal margin; **24**, metatarsal II distal condyles/II-1 proximal articular surface broader in width than metatarsal III/III-1; **25**, metatarsal III medial distal condyle extends significantly ventral to the lateral condyle; **26**, metatarsal IV distal shaft much narrower than metatarsals II and III; **27**, metatarsal IV distal condyles C-shaped in distal view.

Discussion: KUROCHKIN (1996:32-33) listed 34 characters in his diagnosis of Enantiornithes that constitute a mixture of widely cited enantiornithine synapomorphies (e. g., "metatarsal IV reduced" with respect to metatarsal II and III) and symplesiomorphies that characterize many other avians (e. g., "digit I reversed"). KUROCHKIN's list did not introduce any new enantiornithine synapomorphies.

CHIAPPE (1996:213) listed 22 enantiornithine synapomorphies in the most detailed consideration to date. Twelve of these are listed above with revision (1, 3, 7-10, 15, 16, 18, 21, 24, 26). The remaining ten are regarded here as problematic, such as the "concave" superior margin of the humeral head and the "groove" on the shaft of radius. The groove on the shaft of the radius, for

example is also present in the proximate outgroup *Ichthyornis* (MARSH 1880: pl. 30, fig. 4) and may therefore apply to a larger clade.

Sixteen of the synapomorphies listed above are new (2, 4-6, 11-14, 17, 19, 20, 22, 23, 25, 27) and will be described in more detail elsewhere.

*Iberomesornis* SANZ & BONAPARTE 1992

Diagnosis: Same as the species *I. romerali*.

*Iberomesornis romerali* SANZ & BONAPARTE 1992

Holotype: LH 22R, Las Hoyas Collection, Museo de Cuenca, Cuenca Spain.

Revised Diagnosis: Enantiornithine with an elongate pygostyle (75 percent the length of the dorsal vertebral column and femur) and an ischium with a straight and narrow shaft.

Discussion: The original diagnosis for *Iberomesornis romerali* is composed of general statements and observations but does not include any autapomorphies:

"Bird with pectoral region comparable to that of Ornithurae and with the pelvis and posterior limbs similar to that of *Archaeopteryx*. Cervical vertebrae with no traces of neurapophyses. Dorsal vertebrae number 11, with relatively high neural arches and laminar spines. Sacral number five, with hypapophyses. Free caudal vertebrae number eight, with incipient procoely, the three anterior ones with broad transverse processes. Pygostyle laminar, formed of about 10-15 vertebrae. Gastralia absent or vestigial. Coracoid strutlike with a broad sternal expansion for contact for the sternum. Furcula developed with styloid hypocleideum and relatively low clavicular angle. Sternum ossified, articulated with five visible sternal ribs. Humerus/ulna length ratio is 0.94. Proximal and distal tarsals and metatarsals unfused. Hallux reverted, with hypertrophied ungual phalanx." (SANZ & BONAPARTE 1992: 39-40)

SANZ & BONAPARTE (1992) placed *Iberomesornis* within two new higher taxa, Iberomesornithidae and Iberomesornithiformes. As originally proposed, these suprageneric taxa lacked diagnoses and are entirely redundant with the genus *Iberomesornis*. Later MARTIN (1995: 34) grouped two additional genera, *Concornis* (SANZ et al. 1995) and *Noguerornis* (LACASA RUIZ 1989), within these higher taxa, but did not provide any synapomorphies or other justification for this assemblage. These higher taxa, along with many others proposed within Enantiornithes (MARTIN 1995, KUROCHKIN 1996), have yet to be justified by character evidence.

Two features in *Iberomesornis* are interpreted here as potential autapomorphies. The pygostyle is particularly long in *Iberomesornis*, measuring approximately 75 percent of the length of either the dorsal vertebral column or femur. In *Sinornis*, by comparison, the pygostyle is approximately 40 percent the length of the dorsal vertebrae and femur. The pygostyle in most enantiornithines is large compared to euornithine birds, and this may represent the primitive condition for Ornithothoraces. The pygostyle in *Iberomesornis*, however, is particularly long, which is tentatively interpreted here as an autapomorphy.

The straight and narrow shaft of the ischium in *Iberomesornis* is also very different than the posteriorly-curved shafts in *Sinornis* (SERENO et al. in press) and *Concornis* (SANZ et al. 1995) or the deeper, flared ischial shaft in *Ichthyornis* (MARSH 1880).

*Iberomesornis* does not exhibit any diagnostic features in the pes. Referral of an isolated enantiornithine pes from the Las Hoyas deposits to *Iberomesornis* sp. (SANZ & BUSCALIONI 1994) or *Iberomesornis romerali* (KUROCHKIN 1995, 1996), therefore, seems premature, especially given the presence of at least two other enantiornithines in these horizons (*Concornis*, *Eoalulavis*). The bony ungual and its attached claw sheath are very difficult to distinguish in pedes from Las Hoyas, so it is doubtful that minor proportional differences in the ungual of pedal digit I (SANZ & BUSCALIONI 1994) provide a sound basis for taxonomic referral.

### Preservation of the skeleton

The skeleton is preserved resting on its right side. Some crushing and local displacement has occurred, most noticeably in the shafts of the left humerus, radius, and tibiotarsus. The skeleton, nevertheless, remains largely in articulation (Fig. 3). The left scapula maintains its articulation with the coracoid and is only slightly displaced from natural articulation with the furcula. The left glenoid and forelimb, furthermore, are in articulation, and the sternum and ribcage, although flattened, maintain their relations to one another.

The key to understanding the disposition and identification of skeletal parts is to recognize that much of the left half of the skeleton has been sheared and displaced dorsally relative to the right side (Fig. 3). As result, (1) the left sternal and dorsal ribs lie dorsal to their right counterparts, (2) breakage in the left humerus and tibia has shifted the distal portions of each dorsally, (3) the sacrum has rotated into ventral view, and (4) the left pelvic girdle and hind limb have followed the rotation of the sacrum and lie dorsal to their right counterparts.

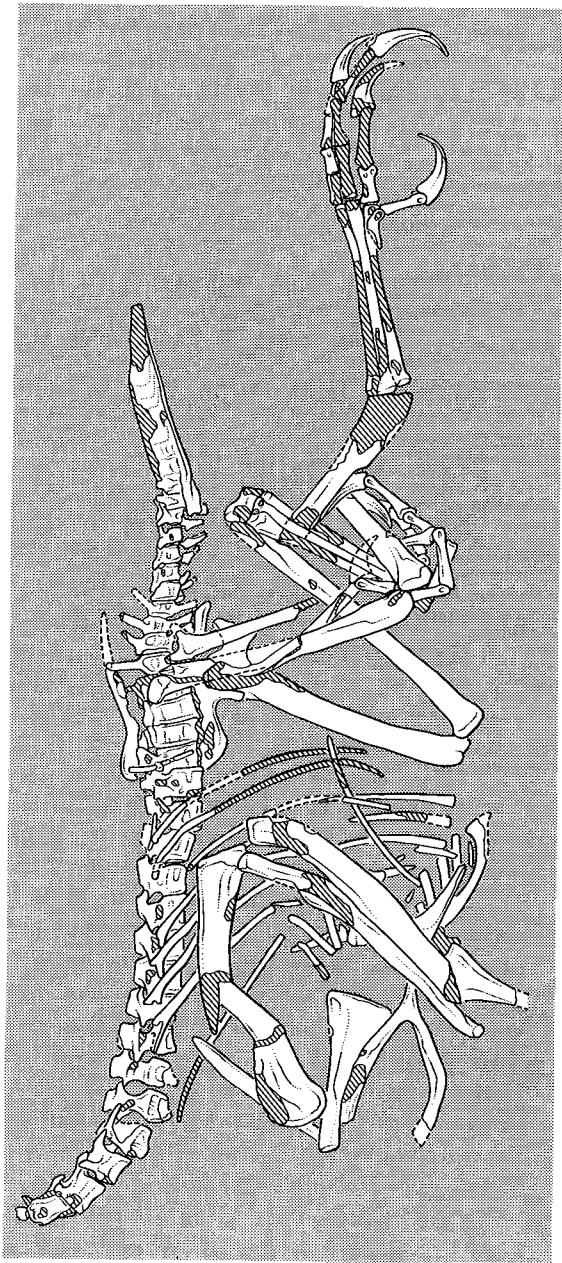


Fig. 3. *Iberomesornis romerali* (LH 22). Skeleton mostly in left lateral view based on camera lucida drawings by the author (Figs. 4-9). Cross-hatching indicates broken bone surface, and dashed lines indicate missing bone margin. Scale bar equals 1 cm.

Some damage has also occurred to the specimen since its original description. The ungual of right pedal digit 1, which was clearly preserved initially (SANZ & BONAPARTE 1992:figs. 1, 3), is now absent (Figs. 3, 8). The outline of this bone is based on the published photographs.

Descriptive - notes

Several bones in the following description are either identified for the first time or given an alternative identification from that given by SANZ & BONAPARTE (1992), as summarized in Table 1. Measurements are given in Table 2.

Vertebral Column

There are four posterior cervical vertebrae preserved, as noted by SANZ & BONAPARTE (1992:40). A fragment of a fifth more anterior cervical is also preserved (Figs. 3, 4). The cervical centra become shorter posteriorly

Table 1. Skeletal identifications of *Iberomesornis romerali* (LH 22) in SANZ & BONAPARTE (1992) compared to those in this paper. Abbreviations: CA, caudal; S, sacral.

SANZ & BONAPARTE 1992	Identifications in this paper
S 1-2	S 1
CA 1-3	S 5-8
anterior portion of pygostyle	CA 5 and 6, chevrons 5 and 6
(no identification)	left lateral process of sternum
right ilium	left ilium
left ilium	right ilium
left femoral head	right femoral head
(not identified)	left femoral head
(not identified)	dorsal process, right and left ischia
(not identified)	right pubis
right tibia, proximal tarsals	right tibiotarsus
left fibula	lateral aspect of the left tibiotarsus
right metatarsals, distal tarsals	right tarsometatarsus
left astragalus	left distal tibiotarsus
(no specific identification)	right metatarsals, phalanges
left pedal phalanx IV-3, IV-ungual	left pedal phalanx III-3, III-ungual
left pedal III-ungual	left pedal IV-ungual
left ribs	left and right ribs

**Table 2.** Measurements in mm of the holotypic specimen of *Iberomesornis romerali* (LH 22). Parentheses indicate estimated measurement. Abbreviations: C, cervical; CA, caudal; D, dorsal; S, sacral. <sup>1</sup> Measurement along dorsal margin of centrum (ventral margin measures 1.3 mm).

Axial column			
Dorsal vertebral column			
Sacrum			
CA 1-6			
pygostyle			
Furcula, dorsolateral ramus			
Hypocleideum			
sternal length (midline)			
?C 6	2.3	S 1	1.4
?C 7	2.2	S 2	1.4
?C 8	1.9	S 3	1.3
?C 9	1.8	S 4	(1.3)
D 1	1.7 <sup>1</sup>	S 5	(1.3)
D 2	1.7	S 6	1.2
D 3	1.7	S 7	1.0
D 4	1.7	S 8	0.9
D 5	1.7	CA 1	0.9
D 6	1.7	CA 2	0.9
D 7	1.7	CA 3	0.9
D 8	1.8	CA 4	0.9
D 9	1.8	CA 5	0.9
D 10	1.7	CA 6	0.8
D 11	1.7		

**Pectoral girdle and forelimb**

Scapula (left)	
length (left)	10.1
width of distal blade	0.8
Coracoid (left)	
length	9.9
width of base	4.2
shaft diameter	1.0
Humerus (left)	
length	(17.6)
Ulna (left)	
length	(19.2)
mid-shaft diameter	1.8
Radius (left)	
length	18.2
mid-shaft diameter	1.0

**Table 2** (continued)  
**Pelvic girdle and hind limb**

Ilium (left)	
length (as exposed)	10.3
Femur (right)	
length	16.4
Tibiotarsus (right)	
length	20.0
Tarsometatarsus (left)	
metatarsal I	2.4
metatarsal II	11.2
metatarsal III	11.8
metatarsal IV	11.5
Pedal phalanges (left)	
I-1	2.9
I-ungual	2.5
II-1	2.3
II-2	3.5
II-ungual	2.2
III-1	3.2
III-2	2.8
III-3	3.4
III-ungual	2.3
IV-1	1.9
IV-2	1.6
IV-3	1.7
IV-4	2.4
IV-ungual	1.8

(Table 2) as in the enantiornithine *Eoalulavis* (Sanz et al. 1996). The centra are very slightly amphicoelous. As in *Eoalulavis*, they exhibit no sign of heterocoely. SANZ & BONAPARTE (1992: 40) reported the presence of “some traces of opisthocoely” in the anterior two centra (reiterated by KUROCHKIN 1995: 51 and CHIAPPE 1996 a: 225), but none can be observed. The centra are excavated laterally with no trace of pneumatic openings, as noted by SANZ & BONAPARTE (1992). A ventral keel is present on the second and third cervical and is extended ventrally as a prominent hypapophysis on the last cervical and anterior two dorsal vertebrae (Figs. 4, 5). The anterior three cervicals lack neural spines, whereas a low rectangular spine is present on the fourth. The postzygapophyses are long and arched throughout the cervical series



with low epipophyses present near their ends in the anterior two cervicals (Fig. 4). SANZ & BONAPARTE (1992: 40) reported the presence of “cervical ribs and fused diapophyses and parapophyses in the last cervicals.” Although no cervical ribs are preserved, breakage near the anterior margin of the cervical centra suggests that partially fused ribs may have been present.

SANZ & BONAPARTE (1992) identified the first dorsal by its distinct form. The centrum is trapezoidal and more strongly excavated laterally. The neural arch is deeper and the more prominent neural spine projects slightly anteriorly. Most importantly, a robust transverse process is present in the middle of the neural arch, which provides a sharp distinction between the cervical and dorsal portions of the axial column in enantiornithines (e. g., *Eoalulavis*) and other ornithothoracines. Eleven dorsals are present as reported by SANZ & BONAPARTE (1992), which is three fewer than in *Archaeopteryx*. If there are nine cervical vertebrae as in *Archaeopteryx* and a recently described enantiornithine from Spain (SANZ et al. 1997), the preserved four cervicals would constitute C 6-9 (Table 2).

The dorsal centra are spool-shaped with parapophyses located on the anterior rim anteriorly but shifting to the middle of the centrum by the mid-dorsals. The transverse processes appear to become shorter and less

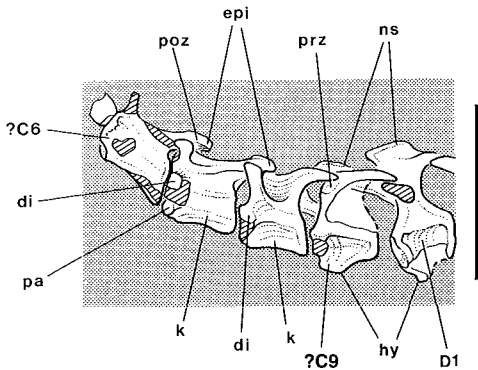


**Fig. 4.** *Iberomesornis romerali* (LH 22). Posterior cervical vertebrae and anterior dorsal vertebrae in left lateral view. Cross-hatching indicates broken bone surface. Scale bar equals 5 mm. Abbreviations: C: cervical vertebra; D: dorsal vertebra; di: diapophysis; epi: epipophysis; hy: hypapophysis; k: keel; ns: neural spine; pa: parapophysis; poz: postzygapophysis; prz: prezygapophysis.

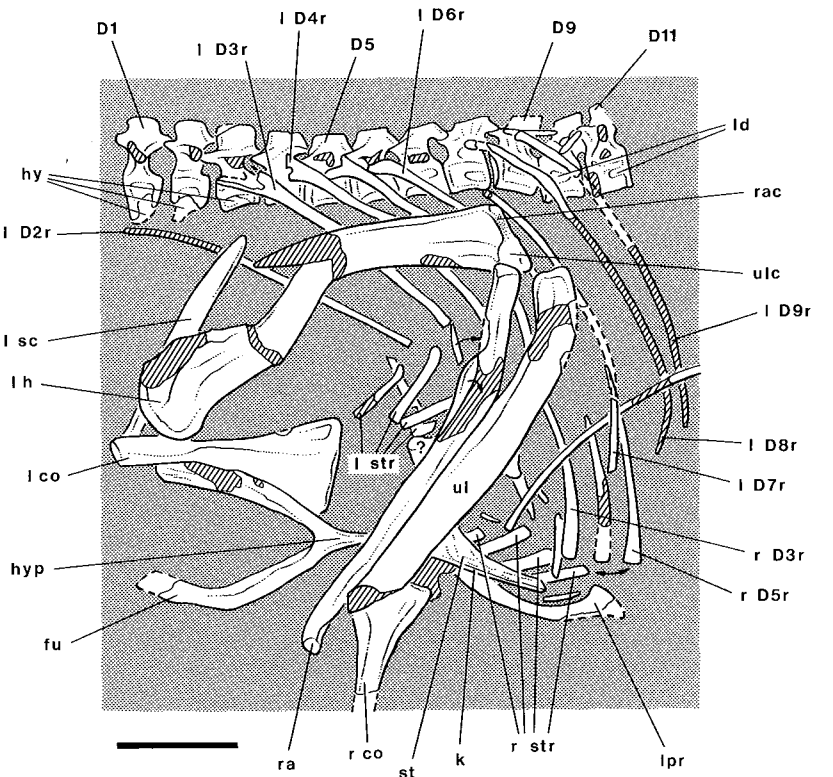


**Fig. 5.** *Iberomesornis romerali* (LH 22). Dorsal vertebrae, ribcage, pectoral girdle and partial left forelimb. Cross-hatching indicates broken bone surface, and dashed lines indicate missing bone margin. Arrows show original position of radial fragments. Scale bar equals 5 mm. Abbreviations: co: coracoid; D: dorsal vertebra; fu: furcula; h: humerus; hy: hypapophysis; l: left; ld: lateral depression; lpr: lateral process; r: rib; r (isolated): right; ra: radius; rac: radial condyle; sc: scapula; st: sternum; str: sternal ribs; ul: ulna; ulc: ulnar condyle.

robust across the dorsal series (Fig. 5). The hypapophyses decrease rapidly in depth from the anteriormost dorsal and disappear by the fifth dorsal. The neural spine remains low and rectangular, decreasing slightly in depth in the posterior dorsals.

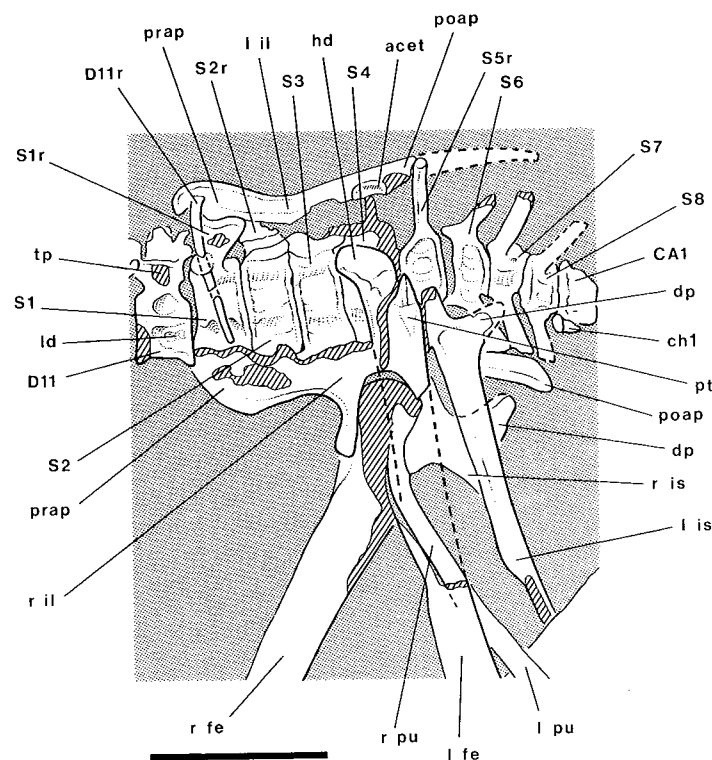


**Fig. 6.** *Iberomesornis romerali* (LH 22). Sacrum, anterior caudals, and pelvic girdle. Cross-hatching indicates broken bone surface, and dashed lines indicate missing bone margin. Scale bar equals 5 mm. Abbreviations: **acet**: acetabulum; **ch**: chevron; **D**: dorsal vertebra; **dp**: dorsal process; **fe**: femur; **hd**: head; **il**: ilium; **is**: ischium; **l**: left; **ld**: lateral depression; **poap**: postacetabular process; **prap**: preacetabular process; **pt**: posterior trochanter; **pu**: pubis; **r**: rib; **r** (isolated): right; **S**: sacral; **tp**: transverse process.

The sacral vertebrae have rotated into ventral view (Fig. 6). As in other enantiornithines such as *Sinornis* (SERENO et al. in press), the sacrum is composed of eight vertebrae, the first three attaching to the preacetabular process, the fourth and fifth attaching over the acetabulum, and the sixth, seventh and eighth attaching to the postacetabular process. The first four sacra appear to be partially coossified, although central sutures are visible.

A low median eminence is present on the first and second sacra. The seventh sacral has a shallow median depression. In the eighth sacral, this depression is deeper and bounded on each side by parasagittal eminences that lead posteriorly to a pair of facets for the first chevron. In the last three sacra (S6-8), the centra decrease in width, so that the width of the last sacral and first caudal centrum are similar. The ribs of the anterior sacra are plate-shaped. The ribs (or transverse processes) of the posteriormost three sacra are much narrower. The fourth sacral is partially obscured by the head of the left femur, but a broken portion of its left rib is exposed above the femur passing laterally to contact the left ilium above the acetabulum (Fig. 6). The ribs (or transverse processes) of S5-8 decrease in length posteriorly as in *Sinornis* (= *Cathayornis*; ZHOU 1995). Their articulation with the postacetabular process of the ilium is best preserved on the right side (Fig. 6). As in the holotypic specimen of *Sinornis* (SERENO et al. in press), the last three sacra (S6-8) have yet to coossify with more anterior sacra, which may indicate immaturity.

SANZ & BONAPARTE (1992) described only five sacra in *Iberomesornis* (Table 1). Their first two sacra actually constitute a single vertebra, the first sacral. They subdivided the first sacral on either side of the shaft of a slender posterior dorsal rib, which came to rest over the centrum. Because they believed the sacra were in lateral view like the remainder of the vertebral column, they misinterpreted the left sacral ribs of the anterior sacral vertebrae as "axial, keel-like ventral processes (hypapophyses)." The presence of eight sacra, rather than five, is supported by the following evidence:

(1) *Preserved location.* If there are eight sacral vertebrae, the sacral series is centered with respect to the pelvic girdle, and the sacral vertebrae are located near appropriate attachment sites on the ilium. S1-3 are located between the preacetabular processes, S4-5 are located near the acetabulum, and S6-8 are located near the postacetabular processes. The five sacral centra described by SANZ & BONAPARTE (1992) all lie anterior to the midpoint of the acetabulum.

(2) *Postmortem displacement.* All eight sacral vertebrae were rotated as a unit to expose their ventral surfaces. The fact that these eight vertebrae rotated along during the dorsal displacement of the left pelvic girdle, while adjacent dorsal and caudal vertebrae remain in lateral view, suggests that they were bound to the pelvic girdle.

(3) *Centrum size and length of ribs/transverse processes.* The centra are broader in S5 and S6 than in the free caudal vertebrae (Fig. 6). If these vertebrae are caudals rather than sacra, there would be an unusual decrease in the width of the centra within the caudal series. The transverse processes

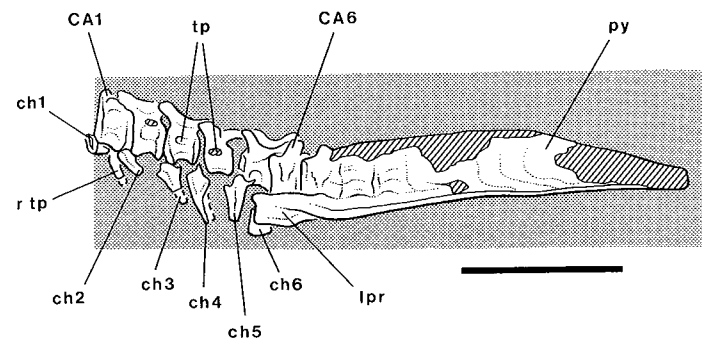


**Fig. 7.** *Iberomesornis romerali* (LH 22). Caudal vertebrae, chevrons, and pygostyle. Cross-hatching indicates broken bone surface, and dashed lines indicate missing bone margin. Scale bar equals 5 mm. Abbreviations: **ch**: chevron; **CA**: caudal vertebra; **lpr**: lateral process; **py**: pygostyle; **r**: right; **tp**: transverse process.

of S6-8 are very long and posterolaterally directed as in S6-8 in *Sinornis* (= *Cathayornis*; ZHOU 1995:fig. 4). In *Iberomesornis* the transverse processes of the free caudals appear to be more reduced, although this may have been exaggerated by breakage.

(4) *Position of first chevron.* The first chevron is located between S8 and CA1, if there are eight sacrals. If there are only five sacrals as originally described, then the first chevron is located in the middle of the caudal series. The first chevron is located between S8 and CA1 in the enantiornithine *Sinornis* (SERENO et al. in press) and the Confuciusornithidae (JI et al. 1999).

(5) *An enantiornithine pattern.* Enantiornithines have eight sacrals and six free caudals, and the first chevron articulates between S8 and CA1 (*Sinornis*; ZHOU 1995; SERENO et al. in press). If there are eight, rather than five, sacrals, this pattern is present in *Iberomesornis*. If there are five sacrals, then *Iberomesornis* has more free caudals (nine) than other enantiornithines and has a more distal position for the first chevron in the middle of the caudal series.

Six caudal vertebrae are exposed in lateral view (Fig. 7). Caudals 1-3 are torqued slightly from lateral view, judging from their prezygapophyses and

chevron facets. There is a slight gap between caudal 4 and 5. Although caudal 5 and 6 are closely associated with the pygostyle, a clear line of matrix separates caudal 5 and 6 and caudal 6 and the pygostyle (Fig. 7). Thus, *Iberomesornis* has the same number of free caudals in the tail as the enantiornithine *Sinornis* (SERENO et al. in press).

SANZ & BONAPARTE (1992:fig. 5), in contrast, used the gap between caudal 4 and 5 to distinguish the free caudals from the pygostyle. Thus their pygostyle is a composite that also includes caudal 5 and 6 and chevron 5 and 6. Because they included several sacrals in the caudal series, they concluded that there are eight, rather than six, free caudals in *Iberomesornis*, and have been followed in this count by PADIAN & CHIAPPE (1988:25).

The free caudal centra are gently amphicoelous and similar in length. The last caudal is slightly shorter than the other free caudals and the succeeding two that form the anterior portion of the coossified pygostyle (Fig. 7). Caudal 2 and 3 have a shallow lateral depression below their transverse processes, which have been broken. Transverse processes appear to be absent in caudal 5 and 6, as in *Sinornis* (SERENO et al. in press). The flat prezygapophyses on several caudals appear to angle ventromedially at about 45°. Caudal 6 has a short postzygapophysis that articulates posteriorly with a facet on the pygostyle. This facet is located on the medial aspect of the anterior end of the keel of the pygostyle, which therefore must be split along this margin into parasagittal laminae. The neural spine is either very low or absent in the anterior free caudals. In caudal 6, a short subrectangular neural spine is present (Fig. 7). The chevrons appear to get longer and broader posteriorly. The last chevron has a rectangular blade that is in contact with the lateral process of the pygostyle.

The pygostyle is very large. It is larger, relative to trunk or femoral length, than in any other enantiornithine. Although thoroughly coossified, the two most anterior vertebrae that have been incorporated into the pygostyle can still be discerned (Fig. 7). The pygostyle has a tall and slightly arched median keel and strong lateral flanges along the ventral margin. The keel tapers in height posteriorly. The lateral flanges are plate-shaped along the length of the pygostyle but extend anteriorly as subrectangular processes in a parasagittal plane lateral to caudal 5 and 6.

## Ribs

SANZ & BONAPARTE (1992:41) remarked that "traces of free ribs" from anterior cervical vertebrae are present, although they did not show them in their figures of the skeleton. If they once existed, none are now preserved. Most of the left dorsal ribs are preserved as well as the distal ends of some of

the right dorsal ribs (Fig. 5). A marked increase in rib length must have been present between cervical and dorsal regions, because the first dorsal rib preserved (for D2) is quite long. Within the dorsal series, it is clear that rib width increases dramatically by the third dorsal rib, and then gradually decreases more posteriorly. This pattern is also seen in *Sinornis* (SERENO et al. in press). The capitulum and tuberculum of the anterior dorsal ribs are separated, but this separation decreases in the mid-dorsal ribs. The posterior dorsal ribs may have been single-headed. The distal ends of the ribs for D3-5 are expanded for articulation with ossified sternal ribs (Fig. 5).

SANZ & BONAPARTE (1992: fig. 5) added the distal ends of the right dorsal ribs to dorsal ribs from the left side, erroneously extending their natural length. Possibly relying on this interpretation, MARTIN (1995:27) noted that *Iberomesornis* was characterized by a "deep ribcage."

Four ossified sternal ribs are present on both sides (Fig. 5). The left sternal ribs are located anterior to the left forearm near their natural articulation with the distal ends of the left anterior dorsal ribs. The right sternal ribs are covered proximally by the sternum. They extend toward the expanded distal ends of the right ribs that probably articulate with D3-5. Four ossified sternal ribs match those in the enantiornithine *Concornis* (LH 2814).

SANZ & BONAPARTE (1992) described five, rather than four, sternal ribs, although they did not identify them on a figure of the skeleton. PADIAN & CHIAPPE (1998: 25) erroneously reported that ossified sternal ribs are absent in *Iberomesornis*.

### Sternum

Part of an ossified sternum is preserved and exposed. A triangular plate appears to represent the posterior portion of the sternum near the midline and appears to preserve a low keel (Fig. 5). Below this plate is a long, curved, and distally expanded lateral process closely resembling that in *Sinornis* (= *Cathayornis*; ZHOU 1995) and *Concornis* (SANZ et al. 1995). This suggests that the remainder of the sternum may have been quite similar in design to that in enantiornithines. The lateral process of the sternum was not described by SANZ & BONAPARTE (1992) (Table 1).

### Pectoral Girdle

The left scapular blade, exposed in lateral view, is narrow and tapers in width toward its distal end (Fig. 5). The left coracoid and distal portion of the right coracoid are exposed in ventral view. As in other enantiornithines, its dorsal surface is deeply hollowed, as seen along cracks in both coracoids. The

lateral margin of the coracoid is straight in *Sinornis* and convex near the coracosternal articulation in *Concornis*. In *Iberomesornis*, the lateral margin becomes slightly convex near the sternal articulation, as best seen on the right coracoid (Fig. 5).

The furcula has broad dorsolateral processes and a long and transversely thin hypocleideum as in other enantiornithines. The broadly separated dorso-lateral processes are L-shaped in cross-section, with the lateral margin of the process deflected posterolaterally. This results in the formation of an elongate trough on the posterior aspect of the dorsolateral process of the furcula that accommodates the medial margin of the coracoid as in enantiornithines. The tip of the right dorsolateral process is preserved and retains its width, unlike confuciusornithids but like enantiornithines.

### Forelimb

The left humerus is preserved in anterior view with its midshaft fractured and distal condyles either distorted or broken away (Fig. 5). Details of the proximal end have been lost in preparation and in breakage along its medial margin. The unusual form of the proximal end of the humerus in enantiornithines, thus, is difficult to assess. Distally, however, the broad width across the condyles and the angled orientation of the distal end closely resemble the condition in enantiornithines. The distal condyles, however, are not well preserved. The radial condyle is crushed flat or broken away so that it appears broader and less prominent anteriorly than the ulnar condyle.

The left ulna and radius, which appear to be slightly longer than the humerus, have proportions similar to basal enantiornithines (Table 3). A section of the radial shaft has been crushed with two fragments rotating anterior to the shaft (Fig. 5, arrows). The distal end of the radius appears to be narrower than the shaft. The ulna is curved proximally. The shaft is twice the diameter of that of the radius (Table 2).

### Pelvic Girdle

The left ilium is better exposed than the right (Fig. 6). The preacetabular process is dorsoventrally broad and somewhat longer than the postacetabular process. A prominent corner marks the junction of the relatively straight ventral margin and the convex anterior margin. The pubic projects ventrally farther than the ischial peduncle, which is hidden from view. The strap-shaped postacetabular process has a posteroventrally beveled posterior margin. SANZ & BONAPARTE (1992: fig. 5) correctly described the general form of the ilium but identified the left ilium as the right and visa versa (Table 1).

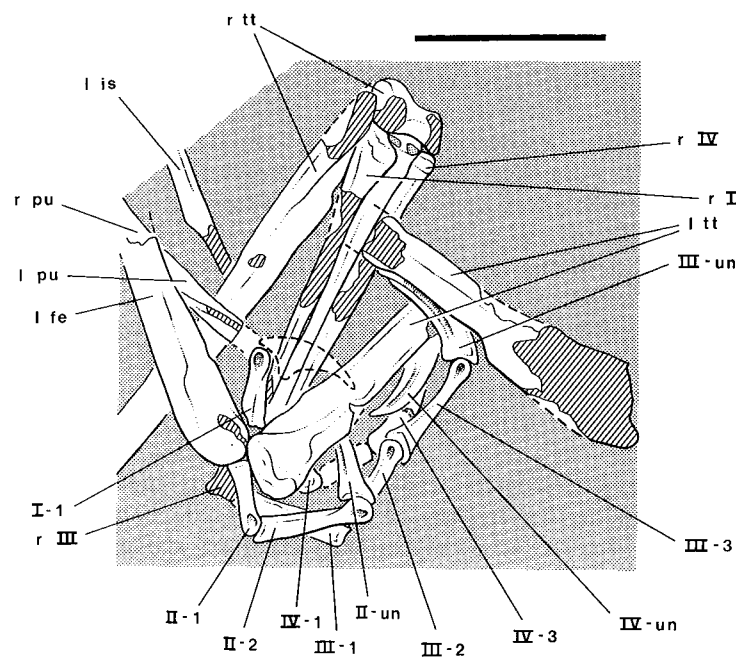


**Fig. 8.** *Iberomesornis romerali* (LH 22). Left and right hind limbs. Cross-hatching indicates broken bone surface, and dashed lines indicate missing bone margin. Scale bar equals 5 mm. Abbreviations: I-IV: digits or metatarsals; 1-3: phalanges; fe: femur; is: ischium; l: left; pu: pubis; r: right; tt: tibiotarsus; un: ungual.

The proximal ends of both ischia are preserved as noted by SANZ & BONAPARTE (1992), and both preserve a dorsal process (Fig. 6). The right dorsal process is very close to its natural articulation with the postacetabular process of the right ilium. The right ischium preserves the peduncular region, which is very broad. The left ischium preserves most of the shaft, which is straight and quite narrow.

Only portions of the right pubis are preserved (Figs. 6, 8). The left femur has been crushed on top of the right pubis, but the pubis is exposed because the mid-shaft of the femur has broken away. This region is very confusing and requires very careful observation. A sliver of the shaft of the left femur

**Table 3.** Comparative ratios of long bones in the holotypic specimens of *Iberomesornis romerali*, *Concornis lacustris*, and *Sinornis santensis*. Measurements for *Sinornis* are from IVPP V9769. Parentheses indicate ratios that are based on one estimated length measurement. Abbreviations; f, femur; h, humerus; mt III, metatarsal III; r, radius; tt, tibiotarsus.

Ratios	<i>Iberomesornis</i>	<i>Concornis</i>	<i>Sinornis</i>
h/r	(0.97)	1.13	1.07
f/tt	0.82	0.69	0.79
tt/mt III	1.70	1.74	1.92
h/f	1.06	1.31	1.14
h + r/f + tt	0.98	1.00	0.98

lies along the anterior margin of the pubic shaft, separated by a line of matrix (Fig. 6). The slender rod-shaped shaft of the right pubis curves postero-ventrally. The distal end of the right pubis continues along the same axis (Fig. 8). In this distal portion of the shaft, a portion of the medially projecting pubic flange is preserved. A portion of this flange is also broken away. If the right pubis is preserved close to its natural orientation relative to the right ilium, then the pubic shaft in *Iberomesornis* was deflected posterior to the vertical. SANZ & BONAPARTE (1992) reported that the pubes are not preserved (Table 3).

**Hind Limb**

The left femur followed the left pelvic girdle that was displaced dorsal to the axial column. Its head is located over the middle sacrals and its mid-shaft is broken away. The length of the left femur matches that for the right femur, suggesting that there was little or no movement of proximal and distal parts despite the breakage and loss of much of the midshaft.

The head slopes ventrolaterally toward the greater trochanter. A bulbous posterior trochanter is located a short distance down the shaft as in *Archaeopteryx* and especially enantiornithines. Although the distal ends of both femora are present, the distal condyles are not well preserved.

The right tibiotarsus is preserved in medial view (Figs. 3, 8). The left tibiotarsus is broken in half; the proximal portion is exposed in lateral view, and the distal portion is exposed in anterior view (Figs. 3, 8). A low

cnemial crest is present on the medial aspect of the proximal end of the right tibiotarsus. The form and position of this crest resemble that in enantiornithines (e. g., *Concornis*; SANZ et al. 1995). The distal end of each tibiotarsus have suffered some crushing and breakage (Fig. 8). The distal articular trochlea is exposed on the right side.

Although SANZ & BONAPARTE (1992: 45) reported the presence of a portion of the left fibula, no part of this bone is preserved. A raised triangular surface on the lateral aspect of the left tibiotarsus may have been misinterpreted as the proximal part of the left fibula. There are no sutures bounding this surface, which is interpreted here as the lateral condyle and lateral aspect of the shaft of the left tibiotarsus (Fig. 8).

SANZ & BONAPARTE (1992) reported the presence of separate astragali and calcanei at the distal ends of both tibiotarsi in *Iberomesornis*.

Although MARTIN (1995: 27) questioned the certainty of this identification, other authors accepted the supposed presence of discrete proximal tarsals as either a sign of immaturity (KUROCHKIN 1995) or an important feature separating *Iberomesornis* from other ornithothoracines (CHIAPPE 1995 a, b; PADIAN & CHIAPPE 1998). Close inspection of these regions does not support these interpretations. The supposed ascending process of the astragalus is based on the distal end of the left tibiotarsus (SANZ & BONAPARTE 1992: fig. 5), which is preserved in cross-section (Fig. 8). Judging from the thickness of the distal end of the left tibiotarsus, the anterior half (including most of the distal condyles) is broken away. A V-shaped edge on this broken surface was identified as the margin of the ascending process of the astragalus (SANZ & BONAPARTE 1992: fig. 5), which was described as "laminar" in form (SANZ & BONAPARTE 1992: 45). Even if this were regarded as an ascending process, its form and presence in *Iberomesornis* are not consistent with information from other avians and avian outgroups. Its low subtriangular form differs from the much taller tongue-shaped process that characterizes *Archaeopteryx* and other nonavian maniraptorans.

The right astragalus was described as "faintly separated from the right tibia" (SANZ & BONAPARTE 1992: 45). This region has also suffered some breakage and crushing from the overlying right metatarsus (Fig. 8).

The distal end shows no clear separation of any element that might be interpreted as an astragalus. The distal condyles do not taper to a thin edge posteriorly, as would be expected in any tetanuran astragalus, and there is no sign of an ascending process anteriorly. If the bone piece that includes the condyles is regarded as an astragalus, it has a very different form than that in *Archaeopteryx* or any tetanuran theropod. A more reasonable interpretation is that the distal end of a completely coossified tibiotarsus has suffered some crushing (Table 1).

SANZ & BONAPARTE (1992: 45) identified a left calcaneum as a "large ossification situated beside the right side of the astragalus", although it was not labeled in their figure of the skeleton (SANZ & BONAPARTE 1992: fig. 5). The region in question, once again, is a broken bone surface at the distal end of the left tibiotarsus that does not show clear separation of accessory ossifications (Fig. 8). *Iberomesornis* is regarded here as having a completely coossified tibiotarsus as occurs in the more basal avian *Confuciusornis*.

Right and left tarsometatarsi are preserved in ventromedial and anterior views, respectively (Figs. 8, 9A). There is no sign of metatarsal V or of separate distal tarsals, which presumably coossified with the proximal ends of metatarsals III and IV. Metatarsals II-IV appear to be coossified at their proximal ends, as best exposed in anterior view of the left tarsometatarsus (Fig. 9A). On the right side, metatarsals II-IV appear to be separate in posterior view (Fig. 8). Thus there is coossification of the proximal end of the tarsometatarsus, albeit of limited extent (contra SANZ & BONAPARTE 1992, KUROCHKIN 1995).

SANZ & BONAPARTE (1992: 45) reported the presence of separate distal tarsals as "two small ossifications above the left metatarsals." There are no ossifications in this region (Fig. 3). A photograph of the right metatarsus under ultraviolet light also appears to show two separate ossifications proximal to metatarsal III (SANZ & BONAPARTE 1992: fig. 3). Close examination of this region reveals that a thin film of matrix covers portions of the proximal end of the tarsometatarsus. The bright areas correspond to exposed areas of the coossified tarsometatarsal cap (Fig. 8). There is no evidence for separate distal tarsals in *Iberomesornis*.

The left tarsometatarsus shows several derived features of enantiornithines. Metatarsal I has a strongly posteriorly reflected distal condyle, (Fig. 9B). A portion of the distal condyle was formerly attributed to the proximal phalanx (SANZ & BONAPARTE 1992: fig. 5). Metatarsal II has the broadest distal condyles. The unusual breadth of these condyles, which are only partially exposed, is confirmed by the broad base of the first phalanx of digit II (Fig. 9B, arrow). The shaft of metatarsal IV is strongly constricted just proximal to the distal condyles (Fig. 9A, arrow). Metatarsal I, in addition, is located near the distal end of the metatarsus, which allows the phalanges of pedal digit I to more directly oppose the phalanges of digits II-IV, as best shown in the enantiornithine *Sinornis* (SERENO & RAO 1992).

The pedal phalanges are best exposed on the left side (Fig. 9B). The proximal phalanx of digit II has a broader base than the others, as noted above. The penultimate phalanges are elongate, although less so in digit IV (Table 2). The large ungual on digit I (now preserved only in the left pes) has a deeper proximal end than the other unguals. The ungual on digit III is the

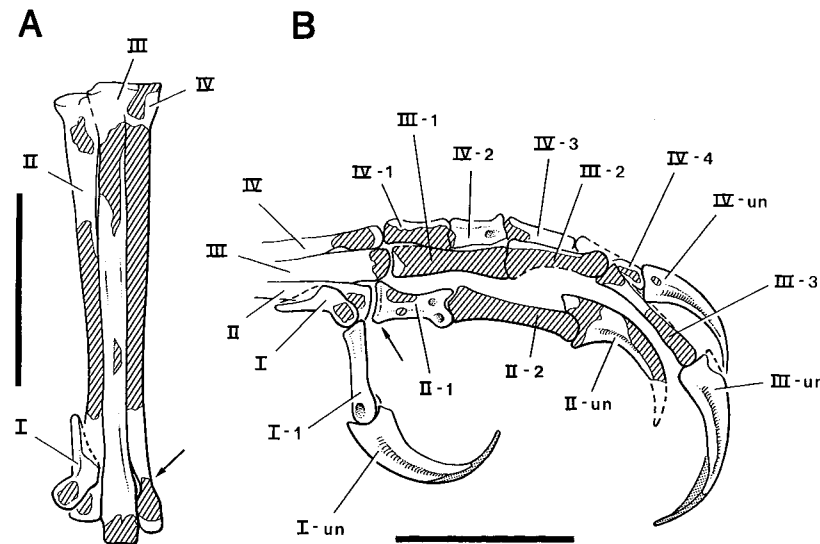


**Fig. 9.** *Iberomesornis romerali* (LH 22). Left tarsometatarsus in dorsal view (A) and left pedal phalanges in dorsal and medial view (B). Cross-hatching indicates broken bone surface, and dashed lines indicate missing bone margin. Arrow (in A) points to constricted distal shaft of metatarsal IV to the expanded base of phalanx II-1. Arrow (in B) points shaded areas at the ends of the unguals indicate the preserved parts of the horny sheath. Scale bar equals 5 mm. Arrow (in A) points to constricted distal shaft of metatarsal IV. Abbreviations: I-IV: digits or metatarsals; 1-4: phalanges; fe: femur; is: ischium; l: left; pu: pubis; r: right; tt: tibiotarsus; un: ungual.

longest pedal ungual. The key to identification of the overlapping bones of the right pes is locating the distal end of metatarsal III, which is exposed at the distal end of the left femur (Fig. 8). The distal condyles are in articulation with the phalanges of digit III. The phalanges of digits II and IV lie above and below those of digit III, respectively.

SANZ & BONAPARTE (1992: fig. 5) confused left pedal digits III and IV where they partially overlap. The proximal two phalanges of digit III were associated with a part of the penultimate phalanx and ungual of digit IV. Likewise, the proximal three phalanges of digit IV were associated with the penultimate phalanx and ungual of digit III, as if these digits crossed one

another, when they do not (Fig. 9B). Their description of a “much shorter” penultimate phalanx and “smaller ungual” in pedal digit III stemmed from swapping the distal parts of digits III and IV. The penultimate phalanx and ungual in digit III are among the longest in the pes, respectively (Table 2).

### *Iberomesornis* - a basal ornithothoracine?

In the initial description of *Iberomesornis*, SANZ et al. (1988) described three features that were remarkably primitive: (1) the presence of only five sacral vertebrae, (2) the lack of fusion between the tibia and proximal tarsals, and (3) the lack of fusion between the distal tarsals and metatarsals. They have been used ever since to distinguish *Iberomesornis* as more primitive than other ornithothoracines (e. g., SANZ & BONAPARTE 1992; SANZ & BUSCALIONI 1992), although the new information given above suggests that these features do not characterize the holotypic skeleton.

Four additional synapomorphies were introduced by SANZ et al. (1995) to unite ornithothoracines more advanced than *Iberomesornis*: (4) heterocoelous cervical vertebrae, (5) scapulocoracoid articulation well below the shoulder end of the coracoid, (6) humeral transverse ligamental groove well developed, (7) humeral distal condyles facing mainly anteriorly (CHIAPPE 1995b). CHIAPPE (1995b) introduced two final synapomorphies to support the same node: (8) prominent ventral processes of the cervicodorsal vertebrae, and (9) fused pelvic elements. Thus a total of nine synapomorphies have been used to unite ornithothoracines to the exclusion of *Iberomesornis*.

Characters 1-3 and 8 are rejected because they are clearly present in the skeleton of *Iberomesornis*. Character 4 (heterocoelous cervical vertebrae) is not present in *Iberomesornis* but also is absent in the posterior cervicals in Enantiornithes. The excellent cervical series in *Eoalulavis* (LH 13500) and the El Montsec enantiornithine (SANZ et al. 1997), for example, demonstrates unequivocally the absence of heterocoely on either side of the centra in the posterior cervicals (the only cervical vertebrae preserved in *Iberomesornis*). Heterocoely in the cervicals in Enantiornithes is limited to the anterior face of anterior mid cervical centra.

Characters 5 and 9 cannot be defended as synapomorphies uniting ornithothoracines to the exclusion of *Iberomesornis*, and CHIAPPE (1996a: 238) sensibly has dropped these from his analysis.

That leaves characters 6 and 7, two features of the humerus. Few details of the proximal end of the humerus are available in *Iberomesornis*. The groove of the transverse ligament across the head of the humerus is marked in *Concornis* and *Eoalulavis* but absent in *Sinornis* (IVPP V9769). Its presence or absence in *Iberomesornis* is speculative (Fig. 5). The disposition of the distal condyles of the humerus are difficult to assess with well preserved



specimens in hand. It is not reasonable to say that the distal condyles in *Iberomesornis* do not face anteriorly and are primitive in this regard (CHIAPPE 1996a: 229), when the radial condyle appears to have been nearly obliterated (Fig. 5). The remains of the ulnar condyle, furthermore, appear to round onto the anterior side of the distal end of the humerus. Thus there does not appear to be any well documented synapomorphies that can unite Enantiornithes and Euornithes to the exclusion of *Iberomesornis*.

### Enantiornithine synapomorphies

Nearly all previous analyses that consider the phylogenetic position of *Iberomesornis* have used Enantiornithes as a terminal taxon and do not test the possibility that *Iberomesornis* might fall within that clade. SANZ et al. (1995) was an exception. In this paper, *Iberomesornis* was scored for 13 enantiornithine synapomorphies. One of these enantiornithine synapomorphies - the broad proportions of the distal condyles of metatarsal II - was scored as present in *Iberomesornis*. One other enantiornithine synapomorphy - a "laterally excavated" furcula - was scored as absent in *Iberomesornis*. As described above, however, this fossa is clearly present on the dorsolateral process of the furcula.

Most of the remaining characters are not considered further here because they are either ill defined or are not present or exposed in a majority of enantiornithine taxa (e. g., "convex external cotyle of ulna," "convex lateral margin of coracoid," "prominent bicipital crest"). Their presence or absence in *Iberomesornis*, in this perspective, is not relevant.

There are ten enantiornithine synapomorphies that are well preserved and exposed in the skeleton (Table 4). The furcular fossa, knife-shaped

Table 4. Enantiornithine synapomorphies in *Iberomesornis romerali* (LH 22)

1. Furcular dorsolateral rami with L-shaped cross-section
2. Hypocleideum knife-shaped
3. Coracoid with posterior fossa
4. Humeral distal condyles, transverse axis ventromedially angled
5. Humeral epicondylar width very broad
6. Iliac postacetabular process very narrow
7. Tibial cnemial crest located anteromedially
8. Metatarsal I distal condyles posteriorly reflected
9. Metatarsal II condyles broad, phalanx II-1 base broad
10. Metatarsal IV distal shaft narrow

hypocleideum, and posterior coracoid fossa are well preserved. The angle and width of the distal humeral condyles resemble the derived condition in Enantiornithes, although the distal end of the humerus is not well preserved. The remaining five enantiornithine synapomorphies are located in the pelvic girdle and hind limb. These are well preserved and easy to verify.

### Conclusions

The skeleton of *Iberomesornis romerali* is remarkably similar to the enantiornithines, *Sinornis santensis* and *Concornis lacustris*. The only features observed here that may constitute autapomorphies for *I. romerali* include the very large size of the pygostyle relative to the trunk or femur and the straight and narrow shaft of the ischium. In this light, reference of an isolated pes from the Las Hoyas beds to *Iberomesornis* (SANZ & BUSCALIONI 1992) or *I. romerali* (KUROCHKIN 1995) is considered premature.

The positioning of *Iberomesornis* as a basal ornithothoracine outside the enantiornithine radiation (SANZ & BUSCALIONI 1992, CHIAPPE 1991, 1995a, b, 1996a, b, 1997, SANZ et al. 1995, 1996, CHIAPPE et al. 1996, PADIAN & CHIAPPE 1998) is based primarily on (1) misidentification of posterior sacra as anterior caudals, (2) misinterpretation of crushed and broken bone at the distal end of the tibiotarsi as separate proximal tarsals, and (3) misinterpretation of the proximal end of the tarsometatarsus as retaining separate distal tarsals. Other synapomorphies that have been proposed to unite ornithothoracines to the exclusion of *Iberomesornis* are rejected, either because they are present in *Iberomesornis* or because they do not characterize ornithothoracines in general.

The enantiornithine status of *Iberomesornis*, on the other hand, is substantiated by ten synapomorphies. *Iberomesornis romerali* provides important evidence regarding vertebral form and number in Enantiornithes. *Iberomesornis*, its contemporaries *Concornis* and *Eoalulavis*, and the Chinese enantiornithine *Sinornis* provide an increasingly detailed picture of the skeletal anatomy of the earliest enantiornithines.

### Acknowledgments

I am indebted to CAROL ABRACZINSKAS for executing the finished illustrations, to JAMES HOPSON, NICHOLAS LONGRICH, HANS LARSSON, and JEFFREY WILSON for review of the manuscript, and to JOSE-LUIS SANZ and ANGELA BUSCALIONI for access to specimens in their care. This research was supported by grants from THE DAVID & LUCILE PACKARD FOUNDATION.



## References

- CHIAPPE, L. M. (1991): Cretaceous avian remains from Patagonia shed new light on the early radiation of birds. – *Alcheringa*, **15**: 333-338; Sydney.
- (1995a): The first 85 million years of avian evolution. – *Nature*, **378**: 349-355; London.
- (1995b): The phylogenetic position of the Cretaceous birds of Argentina: Enantiornithes and *Patagopteryx deferrariisi*. – *Cour. Forschungsinst. Senckenberg*, **181**: 55-63; Frankfurt (Main).
- (1996a): Late Cretaceous birds of southern South America: Anatomy and systematics of Enantiornithes and *Patagopteryx deferrariisi*. – *Münchner Geowiss. Abh.*, **30**: 203-244; München.
- (1996b): Early avian evolution in the southern hemisphere: The fossil record of birds in the Mesozoic of Gondwana. – *Mem. Qsld. Mus.*, **39**: 533-554; Brisbane.
- (1997): Aves. – In: CURRIE, P. J. & PADIAN, K. (Eds.): *Encyclopedia of Dinosaurs*, (pp. 32-38). – San Diego (Academic Press).
- CHIAPPE, L. M. & CALVO, J. O. (1994): *Neuquenornis volans*, a new Late Cretaceous bird (Enantiornithes: Avisauridae) from Patagonia, Argentina. – *J. Vert. Paleont.*, **14**: 230-246; Lawrence.
- CHIAPPE, L. M., NORELL, M. A. & CLARK, J. M. (1996): Phylogenetic position of *Mononykus* (Aves: Alvarezsauridae) from the Late Cretaceous of the Gobi Desert. – *Mem. Qsld. Mus.*, **39**: 557-582; Brisbane.
- CHINSAMY, A., CHIAPPE, L. M. & DODSON, P. (1995): Mesozoic avian bone microstructure: Physiological implications. – *Paleobiol.*, **21**: 561-574; Lawrence.
- FORSTER, C. A., SAMPSON, S. D., CHIAPPE, L. M. & KRAUSE, D. W. (1998): The theropod ancestry of birds: New evidence from the Late Cretaceous of Madagascar. – *Science*, **279**: 1915-1919; Washington, D. C.
- HAECKEL, E. (1866): *Generelle Morphologie der Organismen. Allgemeine Grundzüge der organischen Formen-Wissenschaft, mechanisch begründet durch die von Charles Darwin reformierte Deszendenz-Theorie. II. Allgemeine Entwicklungsgeschichte der Organismen. Kritische Grundzüge der mechanischen Wissenschaft von den entstehenden Formen der Organismen, begründet durch die Deszendenz-Theorie.* – Berlin (Georg Reimer).
- Ji, Q., CHIAPPE, L. M. & Ji, S. (1999): A new Late Cretaceous confuciusornithid bird from China. – *J. Vert. Paleont.*, **19**: 1-7; Lawrence.
- KUROCHKIN, E. N. (1995): Synopsis of Mesozoic birds and early evolution of the Class Aves. – *Archaeopteryx*, **13**: 47-66; München.
- (1996): A new enantiornithid of the Mongolian Late Cretaceous, and a general appraisal of the Infraclass Enantiornithes (Aves). – *Palaeont. Inst., Spec. Issue*: 1-60; Moscow.
- LINNAEUS, C. v. (1758): *Systema Naturae per Raegna Tria Naturae, Secundum Classes, Ordines, Genera, Species, cum Characteribus, Differentiis, Synonymis, Locis.* – (Laurentii Salvii).
- LACASA RUIZ, A. (1989): Nuevo genero de ave fosil del yacimiento Neocomiense del Montsec (Provincia de Lerida, Espana). – *Estud. Geol.*, **45**: 417-425; Madrid.
- MARSH, O. C. (1880): *Odontornithes: A Monograph on the Extinct Toothed Birds of North America.* – (Rept. Geol. Expl. 40th Parallel).

- MARTIN, L. D. (1995): The Enantiornithes: Terrestrial birds of the Cretaceous. – *Cour. Forschungsinst. Senckenberg*, **181**: 23-36; Frankfurt (Main).
- PADIAN, K. & CHIAPPE, L. M. (1998): The origin and early evolution of birds. – *Biol. Rev.*, **73**: 1-42; London.
- SANZ, J. L., BONAPARTE, J. F. & LACASA, A. (1988): Unusual Early Cretaceous birds from Spain. – *Nature*, **331**: 433-435; London.
- SANZ, J. L., CHIAPPE, L. M. & BUSCALIONI, A. D. (1995): The osteology of *Concornis lacustris* (Aves: Enantiornithes) from the Lower Cretaceous of Spain and a reexamination of its phylogenetic relationships. – *Amer. Mus. Novitates*, **3133**: 1-23; New York.
- SANZ, J. L., CHIAPPE, L. M., PÉREZ-MORENO, B. P., BUSCALIONI, A. D., MORATALLA, J. J., ORTEGA, F. & POYATO-ARIZA, F. J. (1996): An Early Cretaceous bird from Spain and its implications for the evolution of avian flight. – *Nature*, **382**: 442-445; London.
- SANZ, J. L., CHIAPPE, L. M., PÉREZ-MORENO, B. P., MORATALLA, J. J., HERNÁNDEZ-CARRASQUILLA, BUSCALIONI, A. D., ORTEGA, F., POYATO-ARIZA, F. J., RASSKIN-GUTMAN, D. & MARTÍNEZ-DELCLÓS, X. (1997): A nestling bird from the Lower Cretaceous of Spain: Implications for avian neck and skull evolution. – *Science*, **276**: 1543-1546.
- SERENO, P. C. (1998): A rationale for phylogenetic definitions, with application to the higher-level taxonomy of Dinosauria. – *N. Jb. Geol. Paläont. Abh.*, **210**: 41-83; Stuttgart.
- SERENO, P. C. & RAO, C. (1992): Early evolution of avian flight and perching: New evidence from the Lower Cretaceous of China. – *Science*, **255**: 845-848; Washington, D. C.
- SERENO, P. C., RAO, C. & LI, J. (in press): *Sinornis santensis* (Aves: Enantiornithes) from the Early Cretaceous of northeastern China. – In: CHIAPPE, L. M. & WITMER, L. M. (Eds.): *Mesozoic Birds: Above the Heads of Dinosaurs*; Berkeley (University of California Press).
- WALKER, C. A. (1981): A new subclass of birds from the Cretaceous of South America. – *Nature*, **292**: 51-53; London.
- ZHOU, Z. (1995): The discovery of Early Cretaceous birds in China. – *Cour. Forschungsinst. Senckenberg*, **181**: 9-22; Frankfurt (Main).

Manuscript received: April 7, 1999.

Revised version accepted by the Tübingen editors: April 30, 1999.

## Address of the author:

Dr. PAUL C. SERENO, University of Chicago, Department of Organismal Biology and Anatomy, 1027 East 57<sup>th</sup> Street, Chicago IL 60637, USA.